High Harmonic Frequency Combs for High Resolution Spectroscopy

A. Ozawa,[1,*] J. Rauschenberger,[1,2] Ch. Gohle,[1] M. Herrmann,[1] D. R. Walker,[1] V. Pervak,[2] A. Fernandez,[1] R. Graf,[2] A. Apolonski,[2] R. Holzwarth,[1] F. Krausz,[1,2] T. W. Hänsch,[1,2] and Th. Udem[1]

[1]*Max-Planck-Institut für Quantenoptik, Hans-Kopfermann-Strasse 1, 85748 Garching, Germany*

[2]*Department für Physik der Ludwig-Maximilians-Universität München, Am Coulombwall 1, 85748 Garching, Germany*

(Received 14 December 2007; published 24 June 2008)

We generated a series of harmonics in a xenon gas jet inside a cavity seeded by pulses from a Ti:sapphire mode-locked laser with a repetition rate of 10.8 MHz. Harmonics up to 19th order at 43 nm were observed with plateau harmonics at the μW power level. An elaborate dispersion compensation scheme and the use of a moderate repetition rate allowed for this significant improvement in output power of the plateau harmonics of 4 orders of magnitude over previous results. With this power level and repetition rate, high-resolution spectroscopy in the extreme ultraviolet region becomes conceivable. An interesting target would be the $1S$-$2S$ transition in hydrogenlike He^+ at 60 nm.

DOI: 10.1103/PhysRevLett.100.253901 PACS numbers: 42.65.Ky, 07.57.−c, 42.60.Da, 42.62.Eh

High-resolution laser spectroscopy has provided us with the most precise measurements in atomic and molecular physics. The $1S$-$2S$ transition frequency in atomic hydrogen, for example, has attained an uncertainty of 1.8 parts in 10^{14}, allowing for important tests of bound state quantum electrodynamics (QED) [1]. Thus far only neutral variants of the most fundamental hydrogenlike systems such as positronium, muonium, and atomic hydrogen can be excited with lasers from the ground state. Much shorter wavelengths, where no lasers exist, are required for charged systems such as He^+, Li^{++}, etc. For the same reason, laser cooling of neutral systems has not been achieved, so that transit time effects are dominating all measurements. On the other hand, hydrogenlike ions, while being more sensitive to higher-order QED contributions, can be held indefinitely at very low temperatures in the virtually undisturbed environment of an ion trap. In fact, the most precise optical frequency measurements are performed this way [2] with complex ions whose properties cannot be predicted from first principles with sufficient accuracy.

Thus far, highly brilliant focusable radiation in the required extreme ultraviolet (XUV) regime can only be generated with large optical bandwidth by synchrotron radiation, free electron lasers or with pulsed four-wave mixing which is notoriously affected by frequency chirps. The process of high harmonic generation (HHG) (see, e.g., [3]) can provide a way out of this dilemma. Even though HHG requires very high laser intensities that can only be reached with pulsed lasers, a coherent XUV pulse train actually consists of a frequency comb of narrow-band laser modes. The mode separation is given by the pulse repetition rate which can be locked to an atomic clock, enabling precise measurement of optical frequencies [4,5]. At the same time the comb modes of the driving laser can be stabilized to a linewidth of a fraction of a hertz [6], just like the best single-mode lasers. Each mode of the frequency comb can therefore be thought of as a continuous wave laser that may be used for high-resolution spectroscopy [7]. In addition, such a frequency comb can cover a large bandwidth with massively parallel acquisition without sacrificing resolution [8,9].

When a two-photon transition, such as the hydrogenlike $1S$-$2S$ transition, is driven with a comb, the modes combine in pairs that add to the same energy. With transform-limited pulses, all transition amplitudes are in phase. The resultant excitation rate is then identical to that of a continuous wave laser of the same average power while maintaining the narrow linewidth [10–12]. In addition, the ac Stark shift is dictated by the average power rather than the high peak power of the pulses [13]. Therefore, direct two-photon frequency comb spectroscopy is essentially equivalent to excitation with a continuous wave laser. The mode number of the XUV comb can be identified using results from hydrogen with the well-known scaling laws or by measuring with at least two different repetition rates [14].

This powerful approach can push high-resolution spectroscopy to shorter wavelengths opening a largely unexplored spectral region [15]. For this to become reality, two main problems had to be solved: The high pulse energies necessary to generate high harmonics could only be provided with low repetition rates, typically in the kHz regime. The resulting frequency comb is far too dense for direct frequency comb spectroscopy which requires the separation of the modes, i.e., the repetition rate, to be larger than the observed transition linewidth. Meanwhile, intracavity HHG achieves the required intensity with the repetition rate of the laser oscillator around 100 MHz [16,17]. This significantly overshoots the design goal. The second obstacle was the very low power generated so far with this method. Now we report a dramatic enhancement of the XUV output power by almost 4 orders of magnitude in the high harmonic plateau, capable of producing useful excitation rates on the $1S$-$2S$ transition of He^+. We achieve this by an elaborate dispersion compensating scheme and by reducing the repetition rate to 10.8 MHz.

Enhancing nonlinear frequency conversion with continuous wave optical cavities is a well-established tech-

nique. To enhance a pulse train in the same way, several additional conditions must be met: (i) Cavity dispersion that is nonlinear in frequency must be minimized so that the pulse shape is preserved upon a round-trip. Interferometric overlap with the driving pulse train is then ensured by (ii) adjusting the cavity length such that the round-trip time matches the repetition period of the laser and (iii) setting the carrier-envelope offset frequency of the laser appropriately. In the frequency domain, the conditions are that the resonant modes of the cavity must be (i) equidistant, (ii) separated by the pulse repetition rate, and (iii) positioned correctly. While the mode spacing and the position of the comb can be adjusted during the experiment, the irregularities of the cavity mode spacing are compensated with chirped dielectric mirrors [18].

We use a Ti:sapphire mode-locked laser that produces a regular comb of continuous wave modes with frequencies $\omega_n = n\omega_r + \omega_{\mathrm{CE}}$. There are two radio frequencies involved: the pulse repetition rate ω_r and the carrier-envelope frequency ω_{CE}. Locking these radio frequencies to a precise reference, such as a Cs atomic clock, establishes a phase coherent connection to the $\approx 2 \times 10^6$ optical frequencies ω_n, due to the large integer $n = 3.4 \times 10^7, \ldots, 3.6 \times 10^7$ [4]. Coupling the frequency comb to the enhancement cavity as sketched in Fig. 1, its nth mode experiences a power amplification of [19]

$$U_n = \frac{T_{\mathrm{IC}}}{1 + A - 2\sqrt{A}\cos(\phi(\omega_n))}. \quad (1)$$

Here, the transmittance of the input coupling mirror is denoted by T_{IC}. The round-trip power factor A is defined as the product of the mirror reflectivities, the input coupler reflectivity and the infrared transmission of the XUV output coupler. The cavity is assumed to have a round-trip length L leading to a round-trip phase shift of the nth mode of $k(\omega_n)L = \phi(\omega_n)$, where $k(\omega_n)$ is the frequency-dependent wave number. The nth mode resonates as

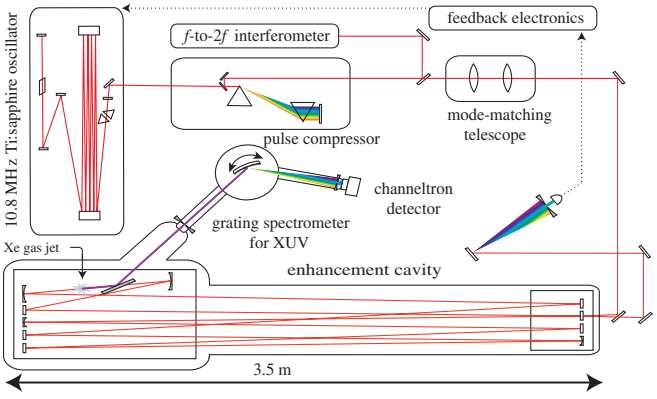

FIG. 1 (color online). Schematic of the setup as described in the text. The f-to-$2f$ interferometer [4] is used to measure intracavity dispersion [22]. The reflection from the cavity is dispersed by a grating to generate an error signal for locking the comb at a specific wavelength.

$\phi(\omega_n)$ becomes an integer multiple of 2π with a finesse $\mathcal{F} \approx \pi/(1 - \sqrt{A})$. The round-trip phase which we express in terms of a power series expansion about some fixed frequency ω_c

$$\phi(\omega_n) = \phi(\omega_c) + \phi'(\omega_c)(\omega_n - \omega_c) + \Delta\phi(\omega_n) \quad (2)$$

needs to be controlled. Without the higher-order dispersion collected in $\Delta\phi(\omega_n)$, all modes may be readily resonated simultaneously by adjusting ω_r and ω_{CE} so that $\omega_r = 2\pi/\phi'(\omega_c)$ and $\omega_{\mathrm{CE}} = \omega_c - \phi(\omega_c)/\phi'(\omega_c)$.

Experimentally these two parameters are controlled by adjusting the laser cavity length and the position of the piezoactuated prismatic wedge in the laser cavity [20]. We find that the drift of ω_{CE} is slow enough that active feedback to the prism position was not necessary for several minutes after optimizing its position manually. The laser cavity length is stabilized by the Pound-Drever-Hall locking method [21]. To generate the necessary modulation sidebands, a small piezoactuated laser mirror is driven at a vibration frequency of 650 kHz avoiding the large dispersion of an electro-optic modulator otherwise used for this purpose. The error signal is processed with a fast proportional and integrating circuit that feeds back on the laser cavity length using two piezoactuators, one with a large bandwidth, the other with a large range. With this approach, a locking bandwidth of more than 100 kHz is achieved.

The phase mismatch $\Delta\phi(\omega_n)$ cannot be controlled by the servo system, so instead we correct it with compensating (chirped) mirrors. The required precision for this dispersion management can be estimated by

$$\Delta\phi(\omega_n) \ll \Delta\phi_{(1/2)} \approx \pi/\mathcal{F}, \quad (3)$$

with $\Delta\phi_{(1/2)}$ being the phase detuning that reduces the power enhancement U_n by one-half. With a constant group delay dispersion (GDD) $\phi''(\omega_c)$ [i.e., $\Delta\phi(\omega_n) = \phi''(\omega_c)(\omega_n - \omega_c)^2/2$], a cavity finesse of $\mathcal{F} = 100\pi$, and a laser bandwidth of 20 THz, $\phi''(\omega_c)$ would have to be smaller than 5 fs^2.

The harmonic radiation is generated at the focus of the cavity in the form of a laserlike beam that propagates collinearly with the infrared laser field. As a consequence, it requires an elaborate outcoupling method. Our solution is to place inside the cavity a sapphire plate, which possesses a refractive index smaller than 1 in the XUV so that total external reflection occurs. By orienting the sapphire plate at Brewster's angle for the fundamental, we introduce minimal cavity loss of about 10^{-3}.

The entire cavity was placed in a vacuum chamber and evacuated to 10^{-2} mbar. This eliminates dispersion and scattering losses from air. The GDD from air amounted to 57 fs^2 in our previous setup [16] and would be 591 fs^2 in our current setup. For the XUV Brewster output coupler, we used a 0.5 mm thick sapphire plate. In our previous setup, the XUV was generated in a tiny vacuum chamber placed at the focus of the cavity with two sapphire win-

dows thick enough to withstand atmospheric pressure. Altogether, we reduced the GDD from 197 fs^2 in our previous 3 m cavity to 34 fs^2 in our 27.8 m cavity. The enhancement cavity consists of 10 mirrors including seven quarter-wave-stack mirrors, four of which are curved, two chirped mirrors, and one input coupler. Asymmetric focusing with two differently curved mirrors (radii of curvature 0.1 and 0.24 m) is used to focus to a waist size of $w_0 = 13\ \mu$m into the gas target. The target is contained within a tube with an inner diameter of 0.4 mm which has been pierced with holes of 200 μm diameter, to allow the laser beam to enter perpendicularly to its axis. At the focus, a peak intensity of $>5 \times 10^{13}$ W/cm^2 is obtained. With a continuous flow of Xe, Ar, or air through the gas nozzle, a fluorescing plasma can be observed. The gas flow is estimated to be 1×10^{-2} mbar l/s.

Two homemade chirped mirrors are used to compensate the dispersion of the Brewster XUV output coupler and the contribution from the other cavity mirrors. First, we designed one chirped mirror by using the estimated total dispersion of the cavity. Then, the residual dispersion is measured by analyzing the spectrally resolved cavity enhancement as described in [22]. Using this information, we generate several different coating designs with the proper dispersion properties. These are optimized by using $\Delta\phi(\omega)$ as a merit function instead of the commonly used GDD. This leaves much more freedom to the actual coating structure, so that more different suitable designs are found. Among these, the one with the smallest sensitivity to coating errors is chosen. To evaluate this sensitivity, we ran a Monte Carlo simulation that adds noise to the layer thickness and recalculates the resulting dispersion properties.

Our mode-locked laser [23] has a 13.9 m long cavity and operates in the positive GDD regime. The cavity is linear and compact due to a Herriott-type multipath delay line. The intracavity GDD of the laser is adjusted by a pair of fused silica prismatic wedges and chirped mirrors. The output of about 1.5 W of average power is compressed by a pair of LaK16 (Schott) prisms. Figure 2 shows the spectrum of this laser and the spectrum of the enhanced pulses. After optimizing the prism compressor, we obtain pulse durations of 38 and 57 fs for the laser and intracavity pulses, respectively, as measured by an autocorrelator, assuming a Gaussian pulse shape.

The intracavity pulse duration is measured using a small residual reflection from the Brewster XUV output coupler. Figure 2 shows that the spectrally resolved power enhancement covers more than 40 nm. We measure 1 W of laser power in front of the cavity, generating 100 W of circulating power, as determined from residual transmission through one of the highly reflecting cavity mirrors. The total power enhancement is only a factor of 2 smaller than the empty, four mirror cavity in [24]. As shown in Fig. 2, a reduced spectral variation of the enhancement was observed when the input pulses were chirped to about 1 ps. This is explained by nonlinear effects due to the high peak intensity at the Brewster XUV output coupler which has a calculated B integral of 1.8 rad. The peak power is around 160 MW.

The XUV output is analyzed by a scanning grating spectrometer (Jobin-Yvon, LHT30) with an estimated resolution of 1.4 nm and a channeltron detector (Burle, CEM4839). The pulse compressor, gas flow rate, nozzle position, and ω_{CE} are optimized to maximize the XUV signal. In order to independently calibrate the XUV power, the (spectrally unresolved) total power is measured with a calibrated Si photodiode (IRD, AXUV20HS1) placed directly after the Brewster XUV output coupler. A 150 nm thick Al filter (Lebow) is used to remove the residual reflection of the fundamental laser beam. The transmission of the Al filter is measured by comparing the XUV spectra with and without it. Together with the specified wavelength dependence of the grating's diffraction efficiency, we recover the true XUV spectrum. After normalizing to the total power, the absolute spectral power density as shown in Fig. 3 is obtained. High harmonics up to the 19th order (41 nm) are clearly observed, which agrees with the calculated cutoff located between the 13th and 15th harmonic.

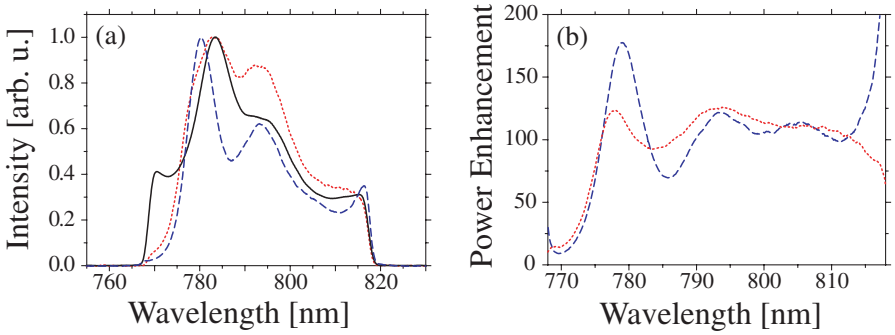

FIG. 2 (color online). Left: The spectrum of the seed laser (solid black curve) together with the intracavity spectrum of a compressed (dashed blue curve) and highly chirped pulse (dotted red curve). Right: Normalizing the intracavity spectra to the seed spectrum and the laser power measured in front of the cavity yields the spectrally resolved power enhancement U_n for compressed (dashed blue curve) and chirped (dotted red curve) pulses. Because of the intensity dependence of $\Delta\phi(\omega)$, the enhancement varies more strongly for shorter pulses.

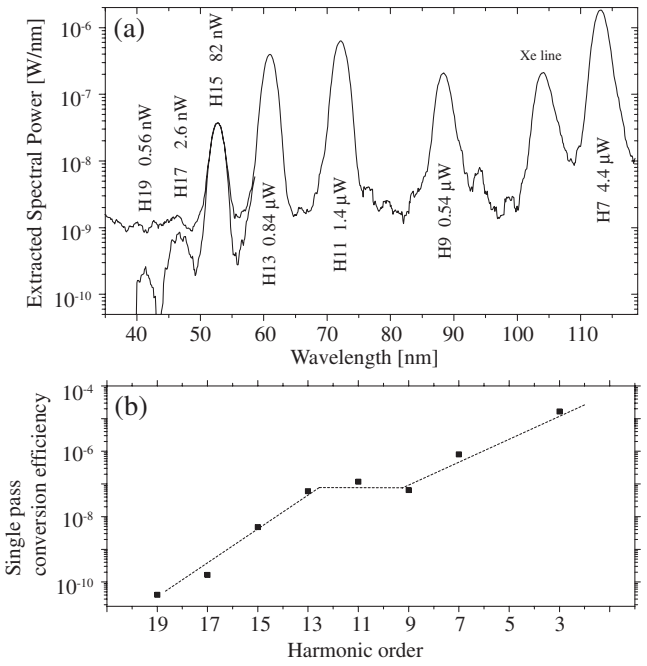

FIG. 3. (a) Spectrum of the outcoupled XUV generated in Xe. Higher harmonics (>H15) are measured with an Al filter to suppress stray light. The spectrally integrated powers for the individual harmonics are given in the plot. Compared to previously reported powers, this represents an improvement of 10^4. (b) The single pass conversion efficiency is derived from the intracavity infrared power for each order of harmonics. The extracted power for H3 is measured with a Si photodiode based power meter.

In addition to the odd harmonics, a broad peak at 104 nm is observed. Its origin is not yet understood but appears to be related to the occupancy of excited bound states of the Xe atom [16].

Two mechanisms are responsible for the drastic improvement over our previous results: larger focal volume and higher peak intensity. The lower repetition rate and the improved cavity lead to a 30-fold increase in pulse energy. The XUV output power scales with large powers of the input power (e.g., $\propto I^9$ for H11 [16]), so even a slightly higher peak intensity leads to significantly higher output power. When saturation is reached, more XUV power is obtained by looser focusing while keeping the peak intensity constant. This lets the interaction volume grow $\propto w_0^4$ and the adverse Gouy phase shift is reduced $\propto w_0^2$. In total, the single pass conversion efficiency for H11 rose from a very low 2×10^{-11} to 10^{-7}. This is a typical value for gas jet HHG without special phase matching measures [3]. We would like to note further that in cavity-assisted HHG the beam quality (due to spatial filtering) is much better than in an amplified system. Therefore, under otherwise identical conditions, we expect higher conversion efficiencies.

With the improvements described here, we obtain μW-level average XUV output power in the plateau region per harmonic. With this power level, precision spectroscopy in the XUV comes into reach for the first time. As an example, a trapped He ion may be excited to the $2S$ state by two-photon absorption using the 13th harmonic at 60.8 nm. A third photon can further ionize to He^{2+}, which can be accumulated in the ion trap and detected with unity efficiency. If the entire 0.84 μW generated so far could be focused on the He ion with a waist size of 0.5 μm, an ionization rate close to 1 Hz could be obtained [25,26]. This is a typical rate for high precision spectroscopy experiments on trapped ions. Such tight focusing has indeed been demonstrated [27]. Delivering the XUV beam from the HHG chamber to the trapped ion with high transmission will require special attention. Since there is virtually no background for this type of detection, we believe precision spectroscopy is realistic even with count rates below 1 Hz.

We thank Dr. Rainer Burhenn of the Max-Planck-Institute for Plasma Physics, Greifswald, Germany for kindly lending us the XUV spectrometer. This research was supported by the DFG cluster of excellence Munich Centre for Advanced Photonics.

Note added in proof.—Since the submission of this manuscript, a μW power level XUV frequency comb was also generated with an Yb fiber laser based system [28].

*akira.ozawa@mpq.mpg.de

[1] M. Fischer *et al.*, Phys. Rev. Lett. **92**, 230802 (2004).
[2] T. Rosenband *et al.*, Science **319**, 1808 (2008).
[3] J. G. Eden, Prog. Quantum Electron. **28**, 197 (2004).
[4] Th. Udem *et al.*, Nature (London) **416**, 233 (2002).
[5] S. Cundiff *et al.*, Rev. Mod. Phys. **75**, 325 (2003).
[6] A. Bartels *et al.*, Opt. Lett. **29**, 1081 (2004).
[7] V. Gerginov *et al.*, Opt. Lett. **30**, 1734 (2005).
[8] S. A. Diddams *et al.*, Nature (London) **445**, 627 (2007).
[9] Ch. Gohle *et al.*, Phys. Rev. Lett. **99**, 263902 (2007).
[10] Ye. V. Baklanov *et al.*, Appl. Phys. **12**, 97 (1977).
[11] M. J. Snadden *et al.*, Opt. Commun. **125**, 70 (1996).
[12] A. Marian *et al.*, Science **306**, 2063 (2004).
[13] P. Fendel *et al.*, Opt. Lett. **32**, 701 (2007).
[14] R. Holzwarth *et al.*, Appl. Phys. B **73**, 269 (2001).
[15] R. Th. Zinkstok *et al.*, Phys. Rev. A **73**, 061801(R) (2006).
[16] Ch. Gohle *et al.*, Nature (London) **436**, 234 (2005).
[17] R. J. Jones *et al.*, Phys. Rev. Lett. **94**, 193201 (2005).
[18] R. Szipöcs *et al.*, Opt. Lett. **19**, 201 (1994).
[19] J. C. Petersen *et al.*, Opt. Express **11**, 2975 (2003).
[20] A. Apolonski *et al.*, Phys. Rev. Lett. **85**, 740 (2000).
[21] R. W. P. Drever *et al.*, Appl. Phys. B **31**, 97 (1983).
[22] A. Schliesser *et al.*, Opt. Express **14**, 5975 (2006).
[23] A. Fernandez *et al.*, Opt. Lett. **29**, 1366 (2004).
[24] I. Hartl *et al.*, Opt. Lett. **32**, 2870 (2007).
[25] M. Haas *et al.*, Phys. Rev. A **73**, 052501 (2006).
[26] M. Herrmann *et al.* (to be published).
[27] H. Mashiko *et al.*, Opt. Lett. **29**, 1927 (2004).
[28] D. C. Yost *et al.*, Opt. Lett. **33**, 1099 (2008).